STUDY OF MAGNETIC CONFINEMENT CONFIGURATIONS FOR FUSION SPACE PROPULSION

A. S. Pagan
Universität Stuttgart
70569 Stuttgart
Germany

E. Ferrer Gil
Universitat Politècnica de Catalunya
08034 Barcelona
Spain

R. A. Gabrielli
Institut für Raumfahrtsysteme
Pfaffenwaldring 29
70569 Stuttgart
Germany

G. Herdrich
Institut für Raumfahrtsysteme
Pfaffenwaldring 29
70569 Stuttgart
Germany

ABSTRACT

Two magnetic confinement concepts, the Spherical Tokamak (ST) and the Field Reversed Configuration (FRC) are evaluated and compared with regards to their performance as core elements of fusion space propulsion systems operating by the working gas drive principle.
To this end, two-dimensional, axisymmetric analytic models for the investigation of the respective magnetic confinement of the fusion plasma are selected, implemented and expanded to include the modelling of thermodynamic plasma quantities and energy transport phenomena. The introduction of a simple fusion criterion allows for the study of local ignition conditions and facilitates the establishment of an energy balance. Burning D-T and D-^{3}He plasmas are considered for both confinement configurations.
An approximate system mass breakdown for each of the proposed thruster systems is presented, exploring the approximate operational system range for both concepts and allowing for a direct comparison with regards to the mass specific power and overall feasibility.
In general, D-T burning working gas fusion propulsion systems are shown to require the use of heavier blankets than comparable D-^{3}He thrusters, making them considerably more massive and severely restricting their practicability due to throwing weight limitations of contemporary launchers.
In direct comparison, the results indicate that a relatively massive fusion propulsion system based on the FRC appears to perform better when operated using the more attainable D-T fusion reaction. Contrastingly, higher mass-specific thrust powers are achieved for the ST when burning the more advanced D-^{3}He reactant couples while also keeping the system mass within acceptable bounds. The absolute and mass-specific thrust powers attainable are shown to be mainly dependent on the system-bound scaling of the energy confinement time τ_E, with smaller values of τ_E permitting higher thrust powers. For the ST, there also appears to be a strong inverse connection between the reactor size and the mass-specific power, prompting the development of small, light-weight fusion propulsion systems to maximise efficiency.

1. INTRODUCTION

As of the early 21st century, one of the most notorious restrictions imposed on extended spaceflight missions is the limited performance of available propulsion systems. Due to physical limitations of thrusters presently utilised, missions to farther destinations such as the outer planets of the solar system come at the cost of a very low available payload mass fraction and/or extensive travel durations. This is especially problematic when a manned mission is envisaged due to the potential hazards attributed to long travel times through space.
A parameter often used to assess the performance of a propulsion system is its mass specific power

$$\alpha = \frac{P_T}{m} = \frac{1}{2} a c_e , \quad (1)$$

where P_T is the propulsive power provided by the system and m is its mass. This parameter can also be expressed through the product of the acceleration a and the exhaust velocity c_e. Assuming a fixed α-value for a given propulsion system, it implies a trade-off between thrust and specific impulse [1]. Present-day propulsion systems may offer high thrust capabilities at a low specific impulse, which is the case for chemical rocket engines, as combustion processes only yield a limited amount of energy to the propellant. On the other hand, electric propulsion systems achieve a high specific impulse and exhaust velocity at a considerable expense of thrust, with material limitations severely restricting the propellant output at any given time.
A propulsion system yielding a high mass specific power with generous limits to both the achievable thrust and the specific impulse would constitute nothing short of a revolution in manned and unmanned space flight, allowing for high payload mass fractions while simultaneously cutting travel times considerably by enabling direct transfer manoeuvres between celestial bodies within the solar system [2].
Nuclear propulsion has been identified as a means of achieving a high mass specific power, making it a viable candidate to bring about this change of paradigm. The most promising practical concept is known as nuclear thermal propulsion, where the heat from the nuclear core is directly used to provide thrust by heating a propellant.
The feasibility and operative range of nuclear fission rockets operating on this principle have been extensively studied, e.g. through the Rover project, resulting in the production and testing of the NERVA rocket engines [3].
While yielding promising results in their own right, nuclear fission rocket engines are expected to be vastly outperformed by nuclear fusion propulsion systems with regards to their efficiency. Fusion propulsion systems yet remain to be developed and constitute the subject of this study.

Nuclear fusion describes the process of two atomic nuclei combining to form the nucleus of a heavier element. Fusing two sufficiently lightweight nuclei releases a considerable amount of energy corresponding to the mass defect between the products and the reactants [4].
Creating enough individual fusion events for practical purposes requires the reactants to be highly energetic. This may be facilitated either through Inertial Confinement, where nuclear fusion is induced by heating and compressing fuel pellets through high-energy beams, or alternatively by confining a highly energetic plasma into a defined reactor volume using powerful magnetic fields [4].
The latter approach is known as magnetic confinement fusion. Recent decades have seen various theoretical and experimental studies of different magnetic configurations which have been deemed practical for the confinement of fusion plasmas, most often with the intention of eventually realising a functioning, sustainable and economically viable terrestrial fusion power plant [5, 6, 7]. The most prominent current fusion research project is the International Thermonuclear Experimental Reactor, or ITER, based on a toroidal magnetic confinement configuration known as the Tokamak [5].
A more compact version of the Tokamak, the Spherical Tokamak (ST) [6] is also being investigated through a variety of projects such as the National Spherical Torus Experiment (NSTX) [8] and has been considered a viable candidate for fusion-powered space propulsion systems [9, 10]. As such, the ST is one of two magnetic confinement configurations examined in this work.
The other concept examined is called the Field Reversed Configuration (FRC) [7]. While it is also a toroidal configuration, it has no central hole, requiring no magnetic field coils running through a central column. Its field lines generate a natural divertor that can be adapted to exhaust plasma particles for space propulsion purposes.
This contribution constitutes a synthesis of two separate efforts with the aim of implementing simple analytic models suited to investigate the ST and the FRC respectively with regards to their potential value as working gas fusion space propulsion systems.
The following section gives an overview of the general requirements imposed on a fusion reactor in space and summarises the basic principles of magnetic confinement within ST and FRC devices. Basic principles regarding the operation of these machines as working gas fusion propulsion systems [11] are outlined. Section **3** discusses the analytical models implemented to describe magnetically confined fusion plasmas in a state of equilibrium within said devices. Results achieved through the application of these models are presented in section **4** and discussed, before drawing conclusions and offering an outlook into future research potential in the final section.

2. SYSTEM CONCEPTS

2.1. General requirements for fusion reactors in space

Regardless of the confinement concept, a variety of specific issues needs to be addressed when attempting to design a space propulsion system based on a fusion reactor:

- The amount of energy yielded by self-sustaining fusion reactors is expected to be abundant. Any excess heat which can not be directed towards heating and exhausting the propellant or recuperated into the fusion plasma must be removed by other means, usually requiring large radiators [9, 11].
- One obvious benefit of operating a fusion reactor in the near-vacuum of space is that no vacuum vessel is required as a prerequisite of generating and sustaining the fusion plasma, as is the case for terrestrial devices such as ITER. This allows for a skeletal design, alleviating the waste heat issue addressed before by allowing highly energetic excess neutrons and bremsstrahlung radiation (see section **3.3**) to escape into free space [9], depending on the desired design specifics.
- The reactor must be able to operate continuously [9].
- The vehicle design must incorporate an independent ability for a reactor start-up, which in practice will likely amount to the inclusion of an auxiliary fission reactor as well as high-performance secondary batteries [9].
- The reactor mass and dimensions of an individual reactor module must be sufficiently small to allow for transport into orbit by available launcher systems, assuming the option of vehicle assembly in space is given [9].
- Considering piloted mission profiles and/or sensitive payloads, some shielding of the crew and said payload from stray radiation may be necessary [11].
- Assuming any kind of nuclear thermal propulsion system, a mechanism by which to efficiently heat the propellant, preferably utilising fusion products and/or reactor waste heat, is required [11].
- Due to thermal limitations of materials, a magnetic nozzle may be required to exhaust ionised propellants and fusion products [9].

2.2 Working gas fusion drives

The working gas fusion drive is an improved variation of the nuclear thermal drive concept. Conventional nuclear thermal propulsion systems such as the fission-based NERVA concept [3] utilise the waste heat of a nuclear reactor core to generate thrust, expanding the heated propellant through a nozzle. However, due to thermal material constraints of the nozzle and reactor components, there exists an upper limit to the propellant temperature, strictly limiting the attainable specific impulse I_{sp} and thus exhaust velocity c_e of such systems. Working gas fusion drives remediate this issue by removing the propellant from direct contact with solid reactor materials prior to it reaching critical temperatures [11]. The magnetic confinement field geometry is then exploited to continue heating the ionised propellant in direct vicinity to the reactor's plasma core before expanding it through a magnetic nozzle. A cross-section of a hypothetical working gas fusion propulsion system utilising a Spherical Tokamak reactor core is pictured in FIG. 1.
The central element of any magnetic fusion propulsion system is the magnetic confinement device supporting the fusion plasma. This requires the use of powerful magnets, providing the magnetic field necessary for confinement. However, further subsystems are essential to ensure the continued operation of the systems discussed in this work.
A generic schematic of the subsystems surrounding the plasma core is given in FIG. 2. The innermost of these subsystems is the blanket, which is situated at the first

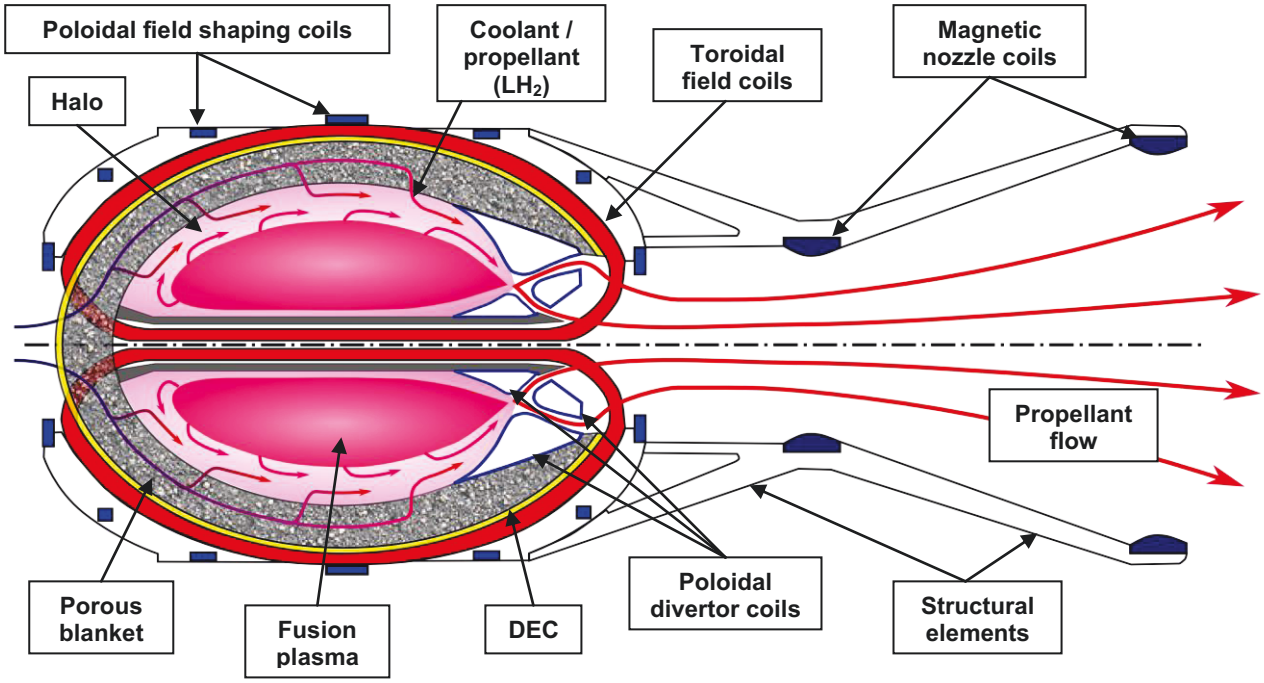

FIG. 1: *Schematic cross section of a Spherical Tokamak working gas fusion propulsion system burning D-^{3}He (Adapted from ref. [9]).*

wall facing the plasma column. One purpose of the blanket is to shield the other (sub-)systems of the spacecraft – potentially including a manned module – from excessive radiation and waste heat generated in the plasma core. Depending on the physical properties of the first wall facing the plasma, some of the radiation emanating from reactor may be reflected back, contributing to the sustainment of the fusion reaction.

The porous blanket allows for a coolant to flow through it, absorbing significant fractions of the waste heat and radiation through convection via the blanket. The liquid coolant – ideally hydrogen due to its excellent caloric properties – vaporises and is seeded out of the blanket into the gap between the reactor's first wall and the plasma core, known as the halo. The coolant proceeds to ionise, thus allowing the reactor's magnetic field prevent it from entering the actual fusion plasma. Fusion products leaking out of the fusion plasma thermalise with the ionised coolant in a magnetic region within the halo called the scrape-off-layer (SOL), heating the coolant further and allowing for a rapid removal of the propellant mixture from the reactor. The particles are then diverted into a magnetic nozzle where they are expanded, thus generating thrust.

Using the coolant as the main component of the propellant allows for an efficient generation of thrust from waste heat while continuously removing a large fraction of it from the spacecraft, greatly relieving the radiators. The working gas drive concept also enables a continuous removal of fusion products, which is necessary to maintain a steady-state operation of the reactor and of the fusion propulsion system as a whole.

A Direct Energy Conversion (DEC) system is installed outside the blanket to further reduce losses and to generate electrical energy, some of which can be used to reheat the plasma core or stored for other purposes.

In order to regulate the temperature of the magnetic coils, which may be required to be superconductive, a cryogenic system is necessary. Any waste heat which is not exhausted with the propellant needs to be removed through radiators [13]. The cryogenic system and the radiators are not pictured in FIGs. 1 and 2.

Some further subsystem requirements, often specific to the magnetic confinement configurations considered in this study, are discussed in the following subsections.

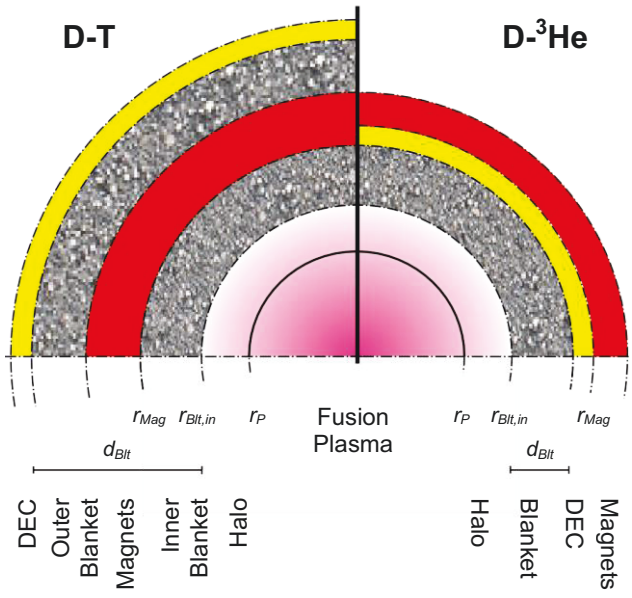

FIG. 2: *Generic diagram of subsystem layers surrounding the fusion plasma core for D-T and D-^{3}He reactant couples.*

2.3 The Spherical Tokamak (ST)

The Spherical Tokamak (ST) configuration, also known as the Spherical Torus, is a variation of the well-studied Tokamak device, the defining difference being the low aspect ratio A, which relates the major radius R_0 to the minor radius a:

(2) $$A = \frac{R_0}{a}.$$

The principle of confinement in an ST is essentially identical to that of a regular Tokamak in that a strong toroidal field is applied through external toroidal field coils. Ions and electrons gyrate around the magnetic field lines, theoretically confining them. However, a variety of loss mechanisms would lead to a rapid loss of confinement, which is countered by a poloidal magnetic field induced by a toroidal electric plasma current I_P. The superposition of both magnetic fields results in magnetic field lines being twisted into a helical shape, along which gyrating plasma particles are constantly shifted around the minor axis of the torus, resulting in a strong confinement [2, 8].
The resulting shape of the plasma resembles a cored apple. A typical schematic outline of an ST plasma column cross section is shown in FIG. 3.
The main advantage associated with STs as compared to regular Tokamaks is an improved confinement efficiency. Weaker magnetic fields are required to maintain a similar degree of confinement, potentially dispensing with the need of superconducting toroidal field coils and greatly reducing the mass and cost of the system in general.
A further desirable effect of the low aspect ratio is that a substantial fraction of the plasma current (the so-called bootstrap current fraction f_{BS}) required to induce the necessary poloidal field for an effective confinement arises automatically within the heated plasma, lowering the requirements for an external current drive [6].
As is depicted in FIG. 1, an ST fusion propulsion system operating by the working gas drive principle could make use of a set of ITER-like poloidal divertors to continuously remove propellant and product particles from the scrape off layer and to divert them towards the magnetic nozzle.
Other approaches to utilise the ST as a propulsion system have been suggested, one being to use divertors to remove energetic plasma particles from the SOL and feeding these to the propellant within a magnetic mixing reservoir directly upstream of the magnetic nozzle [9]. An alternative concept makes use of magnetic field ripples,

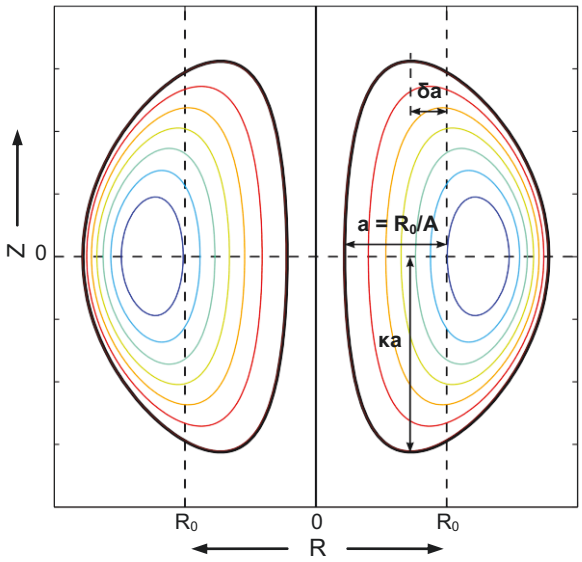

FIG. 3: *Outline of smooth ST plasma column cross section with characteristic magnetic flux surfaces (for Ψ = const.) and definition of geometric parameters (κ: elongation, δ: triangularity).*

causing highly energetic fusion products to be deliberately expelled from confinement into a preferential direction, allowing for a smooth and uninterrupted plasma surface and thus completely dispensing with the need of a magnetic divertor, somewhat simplifying the reactor design [10].

2.4 The Field Reversed Configuration (FRC)

The Field Reversed Configuration (FRC) is a magnetic configuration that can be generated inside a cylindrical coil without the need of invasive toroidal field coils running through the centre of the plasma volume. Configurations such as this, in which there is no central hole, are known as Compact Toroids (CT). A variety of compact toroids can be generated by combining varying components of toroidal and poloidal magnetic fields. The FRC is a particular case of a CT, in which the toroidal magnetic field is negligible in relation to the poloidal field [13].
Due to low magnetic flux densities within the FRC plasma, its stabilisation cannot be explained by using the ideal magnetohydrodynamics (MHD) theory and is instead attributed to non-ideal effects [7].
The absence of a central column and the effectively nonexistent toroidal magnetic field result in a geometric and magnetic simplicity that contribute to making the FRC a promising concept for the confinement of fusion plasmas [13]. The purely poloidal magnetic field results in a very high ratio β between the kinetic pressure and the applied magnetic pressure. In consequence, high plasma pressures can be achieved, allowing highly energetic aneutronic fusion reactions to take place [7].
Two important regions can be distinguished in an FRC, as shown in FIG. 4. In the outer region, the magnetic field lines are open in the domain of observation, i.e., the interior of the magnetic coil. The magnetic field lines are closed within the inner region, allowing for plasma to be confined. The frontier between these two regions is known as separatrix and is central to defining the geometry of an FRC [14]. The separatrix can be defined by its semi-axes *a* and *b*, and by its relative radius, which is the ratio between the semi-minor axis of the separatrix *a*, and the radius of the coil r_c.
The shape of the magnetic field lines outside of the separatrix conveniently result in a natural divertor that can be shaped into a magnetic nozzle, exhausting the fusion products expelled by the plasma together with the heated propellant in order to provide thrust or to generate energy [13].

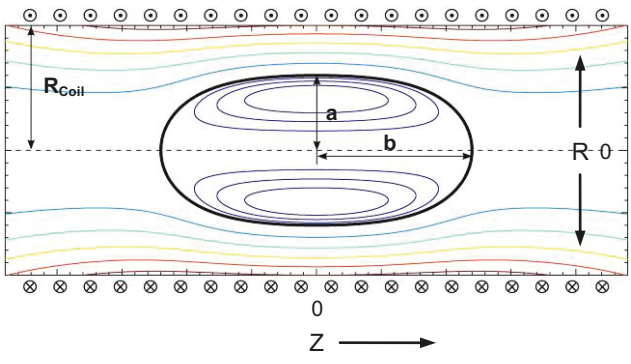

FIG. 4: *Outline of FRC cross section with characteristic magnetic flux surfaces (for Ψ = const.) and definition of geometric parameters (a: minor axis, b: major axis, R_{Coil}: coil radius).*

3. ANALYTIC MODEL

In an attempt to achieve results suitable to compare both systems with regards to their overall performance, a simple analytic model is constructed by combining existing solutions regarding the modelling of the respective magnetic confinement environment with a simple model yielding approximate values of the thermodynamic properties and transport phenomena expected to arise within the fusion plasma.
A coordinate system is defined in accordance with FIGs. 3 and 4. By assuming axial symmetry around *Z*, the problem is effectively reduced to a two-dimensional one.

3.1 Confinement Modelling

The first step in order to model the magnetic confinement environment of both configurations is to obtain a mathematical model of the distribution of the magnetic flux Ψ throughout the fusion plasma. For a 2D system, the magnetic flux function Ψ is required to comply with the Grad-Shafranov (GS) equation. The GS equation describes an ideal magnetohydrodynamic (MHD) equilibrium in a two-dimensional plasma [15] and is given as

$$R\frac{\partial}{\partial R}\left(\frac{1}{R}\frac{\partial \Psi}{\partial R}\right)+\frac{\partial^2 \Psi}{\partial Z^2}=-\mu_0 R^2\frac{dp}{d\Psi}-\frac{1}{2}\frac{dF^2}{d\Psi}, \quad (3)$$

where μ_0 is the vacuum permeability, p is the plasma pressure and $F = RB_\phi$. $B_\phi(R,Z)$ is the toroidal component of the magnetic flux density, which is generated by the toroidal field coils in the ST and negligible for the FRC configuration. Both p and F are considered functions of $\Psi(R,Z)$.
A variety of analytic solutions to the GS equation exist based on different approaches to the problem, often specific to the observed magnetic configuration.
Both solutions selected for modelling the magnetic confinement environment within the ST and the FRC are based on Solov'ev profiles, where p and F are assumed to be in linear dependence of Ψ [16]. While this corresponds to an unrealistic description of the toroidal current profile, which in turn has a detrimental effect on the accuracy of the resulting distributions of p and F, such solutions still retain many crucial physical properties of the configurations in question, are simple to implement and yield fast results [17].
The Spherical Tokamak is modelled using a solution strategy presented in ref. [17]. This solution allows for a full definition of the geometric shape parameters of the fusion plasma column with little or no need to determine operational parameters through iteration. If so desired, single or double x-divertors can be considered in the solution.
The solution selected to model the Field Reversed Configuration is the Steinhauer Analytical Equilibrium [18], which constitutes a superposition of two solutions of the GS equation. The internal solution models the region inside of the separatrix and is based on the Solov'ev solution. It includes a term matching it to an external solution, which models the magnetic configuration outside of the separatrix, fitting it to the cylindrical coil.
Once the magnetic flux function $\Psi(R,Z)$ has been established, both the magnetic flux density distribution $\mathbf{B}(R,Z)$ and the distribution of the plasma pressure $p(R,Z)$ are defined. This allows for the further extraction of plasma figures of merit such as the plasma beta β, which relates the plasma pressure to the magnetic pressure exerted by the magnetic environment. For the sake of brevity, the calculation of these figures of merit will not be discussed here, whereas they are explained in refs. [17] and [18].

3.2 Plasma Performance Model

The ideal gas law applies to a fusion plasma [4]:

$$p = k_B\left(n_e T_e + T_i\sum_{j=1}^{N} n_j\right), \quad (4)$$

with N being the number of individual ion particle species j confined to the plasma volume. n_j is the particle density and the temperature of j, whereas all ion species are assumed to have the same temperature T_i. The electron density and temperature are given through n_e and T_e respectively. k_B is the Boltzmann constant.
Assuming a given temperature distribution, the respective unknown property may be calculated from the pressure p yielded by the confinement solution.
As only charged particles may be influenced through electromagnetic forces, neutral particles such as neutrons are considered to be almost immediately lost from the confinement volume.
The two reactant species' ions are denoted through the indices '*i*' and '*k*' and are usually assumed to exist in identical quantities ($n_i = n_k$).
Neither fusion products, sometimes called ash, nor contamination through heavier ions are considered at any depth for the purpose of this study. However, their effects on the electron and reactant densities are accounted for through simplistic, but nonetheless effective means.
The charge neutrality condition requires that the plasma remains in state of quasi-neutrality by assuring that

$$n_e = \sum_{j=1}^{N} n_j \langle Z_j \rangle , \quad (5)$$

where $\langle Z_j \rangle$ is the average charge state of the ion species j and may be considered equal to its proton number, as most species likely to be encountered in a fusion plasma at temperatures of $T \geq 8$ *keV* are fully ionised [19].
Thus a certain fraction of ash and impurities within the plasma shifts the overall balance towards a noticeable majority of electrons. This is accounted for by simply requiring that

$$n_e = 0.55n . \quad (6)$$

The direct displacement of reactant ions through ash and impurities is approached in a similar fashion, by setting a fixed ratio between the reactant species and electron densities:

$$n_i = n_k = \frac{n_e}{2.5} , \quad (7)$$

with the residual density assumed to be an unspecified composition of ash and impurities.
Other, more sophisticated and accurate ash and impurity models have been implemented, but while eqns. (6) and (7) appear to be overly simplistic, trials in which results obtained using this method were compared to reliable

values from previous works on experimental fusion devices such as JET [20] [21] showed a remarkable agreement. This simple method was thus implemented in an effort to find a common denominator for the differing ST and FRC models, enabling a direct comparison.
Of course, this holds true only when assuming that the rate of ash removal as well as the degree of contamination in an FRC plasma is comparable to that of a (Spherical) Tokamak.
Under the assumption of a similarity to fusion plasmas in regular Tokamaks [5], peaked temperature profiles, often with $T_e \neq T_i$, are assumed for the ST analysis, whereas the corresponding density profiles are comparatively flat. Profiles are prescribed in a "piggy-back" manner by assuming a similar, albeit inverted distribution as the magnetic flux Ψ and exploiting the solution for the flux function accordingly.
For the FRC, a constant temperature $T_e = T_i = const.$ is assumed throughout the plasma volume, based on observations made in previous studies of experimental FRC confinement devices [22]. The shape of the resulting density profiles thus resembles the pressure profile yielded by the confinement solution.
Once the individual particle density and temperature distributions have been established, energy transport phenomena may be modelled. Ref. [12] presents expressions enabling the calculation of the fusion power $P_F = f(n_i,n_k,T_i)$, the thermal losses $P_{th} = f(n,T,\tau_E)$ and the Bremsstrahlung and Synchrotron radiation losses, $P_{BrS} = f(n_e,n_i,n_k,n_{ash},T_e)$ and $P_{Syn} = f(n_e,T_e,B)$, respectively, for a generic 0D fusion reactor. τ_E is the energy confinement time, which is approximated individually for the ST and the FRC in accordance with literature data [22] [23] (see also section **4.3**).
The transport power expressions can be adapted for the multidimensional model by applying the formulae to all discrete data points and numerically integrating the thus obtained power density values over the whole of the plasma volume utilising the Guldinus theorem. As an example, the total fusion power $P_{F,tot}$ is obtained thus:

$$P_{F,tot} = 2\pi \int_A \frac{n_i n_k}{1+\delta_{ik}} \langle \sigma v \rangle E_F R dA \,. \tag{8}$$

A represents the area of the plasma column's cross section and δ_{ik} is Kronecker's delta, preventing identical reactants from being counted twice. $\langle \sigma v \rangle$ is the thermal fusion reactivity, which is calculated in dependence of T_i and in accordance with ref. [24]. E_F represents the energy released through an individual fusion event.

3.3 Lawson Criterion

A generic energy balance equation is established in ref. [12]. Its time derivative is

$$P_G + P_R = P_L \,, \tag{9}$$

whereas P_G, P_R and P_L refer to the power gained, recycled and lost, respectively.
The energy transport expressions are multiplied with individual feedback fractions k_{back} for those power losses which may be partially recuperated through reflective walls or other means in order to reheat the plasma. After substituting these expressions into the energy balance eqn. (9) and rearranging the result, the generalised burn criterion is obtained:

$$n_i \tau_E T_i = \frac{3}{2} \frac{(1-k_{back,th}) k_B T_i^2 \Psi_{tot}}{\Omega_F - \Omega_{BrS} - \Omega_{Syn}} \,. \tag{10}$$

Here, Ψ_{tot} is a particle multiple, relating the sum of all confined particle densities to the first species reactant density n_i while also compensating for temperatures deviating from T_i. The abbreviation Ω_F represents the power gain through fusion processes, while Ω_{BrS} and Ω_{Syn} represent the losses through bremsstrahlung and synchrotron radiation. The parameter $k_{back,th}$ is the thermal feedback factor, while the equivalent factors pertaining to the recuperation of neutron power and radiation are included in the abbreviations Ω. Moreover, $n_i \tau_E T_i$ is known as the triple product and is supplied by the plasma performance model for every discrete point throughout the plasma volume. The right-hand side of eqn. (10) is evaluated accordingly.
The result may be interpreted in that all regions in which the burn criterion is exceeded may be regarded as contributing to the net power obtained from the reactor, whereas the areas where the criterion is not met are essentially losing power. However, bearing in mind that eqn. (10) has been adapted from a generic 0D model, this corresponds to the potentially unrealistic case in which recuperated power loss fractions are fed back directly into their point of origin.

4. ANALYSIS

4.1 Fuel selection considerations

A variety of nuclear fusion reactions of different reactant pairings have been considered for application in reactors and propulsion systems [11]. The use of two distinct fuel pairings is considered in this work, both of which are considered the most likely candidates for the realisation of working fusion reactors within the foreseeable future:

$$D + T \rightarrow n^0 + {}^4He$$
$$D + {}^3He \rightarrow p^+ + {}^4He$$

The first fusion reaction, referred to here as the Deuterium-Tritium or D-T reaction, imposes relatively low requirements on the reactor system with plasma temperatures around 10 *keV* usually being sufficiently high for a sustained reaction. This makes it the fusion reaction of choice for many conceptual and experimental terrestrial fusion devices such as JET [20] and ITER [5]. The supply of fuel components is considered ample. However, since a considerable fraction (approx. 80%) of the fusion power is yielded to the produced neutrons, shielding of the payload and of reactor materials prone to radioactive activation through neutrons are of considerable concern, often requiring an excessive amount of additional mass. [11, 12] Furthermore, as the neutrons can not contribute to the reheating of the fusion plasma, some additional external plasma heating may be required, further complicating the system.
The Deuterium-Helium-3 (D-^{3}He) fusion reaction greatly alleviates this problem, as neutrons are produced merely in a side reaction (not shown here) at a fraction of approx. 5%, thus considerably reducing the shielding and probable reheating requirements. However, temperatures of around 100 *keV* are required to sustain such a reaction, imposing

high requirements on the effectiveness of the magnetic confinement. Helium-3 (^{3}He) is considered to be extremely rare and difficult to obtain in significant quantities on Earth, while abundant supplies are expected to be found elsewhere in the Solar System, most notably on the Moon and the gas giants.
Further, more advanced fusion reactions yielding few or no neutrons have been considered for fusion space propulsion systems:

$$^{11}B + p^+ \rightarrow 3\,^4He$$
$$^3He + {}^3He \rightarrow 2p^+ + {}^4He$$

However, the requirements imposed on adequate magnetic confinement systems are immense. Early trials conducted for this work have suggested that the magnetic flux densities required to uphold the necessary plasma pressures would cause excessive energy losses through bremsstrahlung radiation, surpassing even the energy gained through the fusion reaction. Thus, no analysis was conducted incorporating these advanced reactant pairings.

4.2 Design point selection

The ST and the FRC propulsion systems are compared by determining the range of the mass specific power α that can be achieved under practical circumstances. Reactor design points are selected both for D-T and for D-^{3}He reactions with the intention of encompassing the respectively largest possible range of operation. The volume-averaged net power P_{net} of the propulsion system is zero, which corresponds to the case in which the Lawson criterion eqn. (10) is met for the plasma volume as a whole. A practicable fusion propulsion system would operate close to this point without exceeding it, thus guaranteeing a mostly self-sustaining fusion reaction while retaining full control over the reactor.
The working gas drive concept applied to both confinement configurations considered in this study requires the absorption of much of the waste energy emitted in the form of electromagnetic radiation and neutrons by the plasma column within the blanket [12]. All of the thus absorbed waste energy is assumed to be efficiently used to preheat the coolant conductively prior to it being seeded into the halo. A significant fraction of the thermal losses, however, are absorbed by the preheated coolant within the halo before reaching the blanket.
The maximum heat and neutron loads $Pb_{th,max} \approx 5\text{MW/m}^3$ and $Pb_{n0,max} \approx 20\text{MW/m}^3$ are not to be exceeded at the first wall for any configuration, effectively enforcing a lower limit with regards to the reactor size, as wall loads grow with a reduced plasma volume. For added safety, the thermal loading at the first wall was asserted disregarding the prior heat absorption by the coolant within the halo.
Parameters concerning the recuperation of energy losses such as wall reflectivities and blanket absorption efficiencies for the individual energy loss phenomena are prescribed at common values as given in ref. [12] so as to simplify a direct system comparison. The power gain Q is set to $Q \rightarrow \infty$, assuming a fully self-sustaining reaction.
The Spherical Tokamak system design evaluated here is based on the ARIES-ST reactor study [25]. While maintaining identical geometric and magnetic confinement field proportions, the desired design points were met by rescaling both the volume of the plasma column and the toroidal vacuum magnetic flux density B_0. The corresponding energy confinement time τ_E is calculated using the adapted ITER-89P scaling mode as given in ref. [23]. A normalisation towards the baseline values of the

Fuel	**D-T**			**D-^{3}He**		
A	1.60					
κ	3.40					
δ	0.64					
R_0 / m	**0.6**	**1.6**	**2.2**	**1.6**	**2.2**	**2.7**
V_{Plasma} / m^3	4.80	91.1	237	91.1	237	438
B_0 / T	4.31	2.21	1.78	6.37	5.13	4.46
I_P / MA	11.2	15.3	16.9	44.0	48.7	52.0
f_{BS} / %	84.5					
β_t / %	50					
q_a	12.2					
<T> keV	16			50		
T_0/<T>	2					
<n_e> /$10^{20}m^{-3}$	7.13	1.88	1.22	4.98	3.23	2.44
n_0/<n>	1.26					
τ_E / s	0.30	1.14	1.76	1.49	2.30	3.04
$P_{F,tot}$ / MW	456.0	600.3	656.2	904.2	989.5	1046
$P_{th,tot}$ / MW	88.7	116.8	127.7	737.7	807.0	853.9
$P_{BrS,tot}$ / MW	4.87	6.40	7.00	190.2	208.1	220.1
$P_{Syn,tot}$ / MW	0.08	0.11	0.12	8.75	9.57	10.1
P_T / MW	430.6	566.7	619.5	835.6	914.1	967.1
Pd_{n0} / MWm^{-2}	16.1	2.99	1.73	0.28	0.16	0.11
Pd_{th} / MWm^{-2}	3.93	0.73	0.42	4.59	2.66	1.87

TAB. 1: *Geometric and operational parameters for a Spherical Tokamak (ST) fusion propulsion system reactor.*

Fuel	**D-T**			**D-^{3}He**		
L_{Coil} / m	**10.8**	**20**	**20**	**9**	**20**	**20**
R_{Coil} / m	**2**	**2**	**3**	**1.5**	**1.5**	**2**
a / m	0.72	0.72	0.6	0.6	0.6	0.46
b / m	3.6	6.67	6.67	3	6.67	6.67
V_{Plasma} / m^3	9.32	17.36	12.06	5.40	12.1	7.09
B / T	4.50		5.11	8.41		10.19
β / %	91		97	89		96
<T> keV	23.7			110.4		
T_0/<T>	1					
<n_e> / $10^{20}m^{-3}$	10.6		14.7	7.78		12.37
n_0/<n>	1.10		1.03	1.13		1.04
τ_E / s	0.21		0.15	0.84		0.53
$P_{F,tot}$ / MW	2654	4762	6287	284	636	940
$P_{th,tot}$ / MW	493	955	1209	239	536	893
$P_{BrS,tot}$ / MW	21	39	52	36	80	118
$P_{Syn,tot}$ / MW	0.02	0.03	0.01	0.19	0.43	0.20
P_T / MW	2409	4476	5909	258	576	852
Pd_{n0} / MWm^{-2}	20		16	0.25		
Pd_{th} / MWm^{-2}	4.56		4	5		

TAB. 2: *Geometric and operational parameters for a Field Reversed Configuration (FRC) fusion propulsion system reactor.*

ARIES-ST study yields

$$\tau_{E,ST} = 2.14184s \cdot \left(\frac{I_P}{28.49MA}\right)^{0.85} \cdot \left(\frac{B_0}{2.08T}\right)^{0.2} \cdot \left(\frac{\langle n_e \rangle}{1.58 \cdot 10^{20} m^{-3}}\right)^{0.1} \cdot \left(\frac{R_0}{3.2}\right)^{1.5} \cdot \left(\frac{P_{TR}}{744.3MW}\right)^{-0.5} . \quad (11)$$

P_{TR} is the total of the power required to reheat the plasma. This scaling law applies only to ST reactors of identical geometric proportions as ARIES-ST. For simplicity, similar or identical operational parameters to those given for ARIES-ST are prescribed where possible.

Operational boundaries such as the Greenwald density limit [26] were not exceeded. An effective upper limit to the reactor size was somewhat arbitrarily enforced by not allowing the propulsion system diameter to exceed a total value of D_{tot} = 12*m*, catering to a generous upper limit of contemporary launcher capabilities. The most prominent geometric and operational parameters for the proposed ST propulsion system are given in TAB. 1.

The FRC configurations given in TAB. 2 have been selected by taking into account that higher values for the specific power can be achieved with minimal core radii. However, a minimum value of the coil radius below which it is impossible to operate the FRC without exceeding the physical limitations of the first wall exists and was taken into consideration. The length of the magnetic coils has been constrained to a maximum value of 20*m* due to space launch system limitations. The size of the separatrix inside the coil has been optimised for maximum power generation without exceeding the physical constraints.

The energy confinement time scaling law for the FRC propulsion system is determined in analogy to the ST by normalising the scaling law provided by ref. [22] to the ARTEMIS-L fusion reactor study, obtaining

$$\tau_{E,FRC} = 6.7s \cdot \left(\frac{a}{1.68m}\right)^{2.7} \cdot \left(\frac{B}{5.36T}\right)^{1.35} \cdot \left(\frac{\langle Z \rangle}{1.5}\right)^{1.35} \cdot \left(\frac{T}{83.5keV}\right)^{0.325} , \quad (12)$$

where <*Z*> is the average proton charge number of the reactants. It is assumed that the volume-averaged magnetic flux density within the separatrix <*B*> roughly scales proportionately to the externally applied field *B*.

While the criteria concerning the power output of both the ST and the FRC propulsion system may be satisfied with a variety of configurations, some of which may prove more efficient than the designs discussed here, the given configurations can be regarded as typical examples of the respective systems.

4.3 System mass model

A simplistic mass approximation model [12] is applied to the individual design points of the ST and the FRC propulsion systems, covering the subsystems described in section **2.2**, however neglecting other essential components such as an auxiliary fission reactor, secondary batteries, plasma heating and current drive systems, plasma refuelling mechanisms as well as the magnetic nozzle, fuel storage and structural elements. Neither is the remainder of the vehicle mass considered. It is assumed that, for a similar performance, the respective masses of the neglected systems scale independently from the utilised fusion reactor system or can be neglected with little error.

FIG. 2 displays the layering of the subsystems encompassing the plasma core for both reactant couples considered.

The inner (local) radius of the blanket $r_{Blt,in}$ is assumed as $r_{Blt,in}$ = 1.25 r_P, whereas r_P is the local radius of the separatrix. The thickness d_{Blt} of the blanket and thus the outer radius are subject to shielding considerations. As the penetration depth of electromagnetic radiation into a given material is regarded as being considerably lower than for neutron radiation, the thickness of the blanket is determined by the requirement of absorbing ≈ 95% of the neutrons emanating from the plasma core for a D-T reaction. The thickness is accordingly set to d_{Blt} =1.5*m* [12].

In contrast, the D-^{3}He reaction yields a considerably lower quantity of neutrons due to a side reaction which has been neglected earlier on in this study. The blanket thickness is set to d_{Blt} = 0.5*m* [12], allowing it to absorb ≈ 70% of the neutrons while keeping the overall system mass low.

The mass of the blanket can be approximated as follows:

$$m_{Blt} = \rho_{Blt} V_{Blt} (1 - k_{Por}) , \quad (13)$$

ρ_{Blt} is the density of the blanket material, which is assumed to be made of SiC with ρ_{Blt} ≈ 4000 *kg/m³*. SiC is considered to be highly resistive against radioactive activation [12, 27]. The porosity of the blanket is considered via the volume fraction k_{Por} = 0.66.

The volume of the blanket is dependent on the shape of the fusion plasma it encompasses. While a simple cylindrical approximation is used for the FRC, the ST blanket is assumed to resemble a prolate spheroid, neglecting the narrow central column running through the plasma toroid, which generally allows only for a limited blanket or shield thickness. The shielding of the central column itself must, however, be sufficiently thick to effectively reduce the neutron load on the inboard toroidal field coils to an acceptable level, thus likely increasing the minimum size for a feasible ST fusion propulsion system when using D-T reactants. Neglecting the surface area of the central column when calculating the wall loads may alleviate this issue to some extent. The system mass analysis in general is also simplified with relatively little error by neglecting the volume and mass of the central column.

When calculating the blanket volume for a D-T reactor, the embedded magnetic field coils are not assumed to influence the blanket thickness d_{Blt} (see FIG. 2).

The masses of the DEC m_{DEC} and of the radiators m_{Rad} are proportionate to the waste heat P_{Waste}, which corresponds to the residual energy flux that has passed through the blanket without being absorbed:

$$m_{DEC} = \frac{\eta P_{Waste}}{\alpha_{DEC}} , \quad (14)$$

and

$$m_{Rad} = \frac{(1-\eta) P_{Waste}}{\alpha_{Rad}} . \quad (15)$$

Here, η represents the efficiency of the DEC and is assigned a value of η = 0.06. α_{DEC} = 569 *W/kg* and

Fuel	D-T			D-^{3}He		
R_0 / m	**0.6**	**1.6**	**2.2**	**1.6**	**2.2**	**2.7**
D_{tot} / *m*	5.44	9.50	11.94	7.1	9.54	11.57
m_{Blt} / *t*	116.8	483.3	825.6	70.93	131.1	195.3
m_{DEC} / *t*	2.86	3.76	4.11	7.78	8.51	9.00
m_{Rad} / *t*	0.85	1.12	1.22	2.31	2.53	2.68
m_{Mag} / *t*	0.96	2.73	4.14	19.4	30.6	41.4
m_{Cryo} / *t*	0.32	0.91	1.38	6.45	10.2	13.8
m_{tot} / t	121.8	491.8	836.5	106.7	183.0	262.2
P_T / MW	430.6	566.7	619.5	835.6	914.1	967.1
α / W kg^{-1}	3536	1152	740.6	7821	4996	3688

TAB. 3: *Diameter, system mass breakdown and performance of the Spherical Tokamak (ST) fusion propulsion system.*

Fuel	D-T			D-^{3}He		
L_{Coil} / m	**10.8**	**20**	**20**	**9**	**20**	**20**
R_{Coil} / m	**2**	**2**	**3**	**1.5**	**1.5**	**2**
m_{Blt} / *t*	311.4	576.8	833.1	167.0	371.2	519.7
m_{DEC} / *t*	16.00	29.73	39.25	2.60	5.82	8.61
m_{Rad} / *t*	4.75	8.83	11.7	0.77	1.73	2.56
m_{Mag} / *t*	5.46	10.12	29.14	8.95	19.88	51.91
m_{Cryo} / *t*	1.82	3.37	9.80	2.98	6.63	17.30
m_{tot} / t	339.5	628.8	923.3	182.3	405.2	600.0
P_T / MW	2409	4476	5909	258	576	852
α / W kg^{-1}	7095	7118	6400	1414	1422	1420

TAB. 4: *Dimensions, system mass breakdown and performance of the Field Reversed Configuration (FRC) fusion prop. system.*

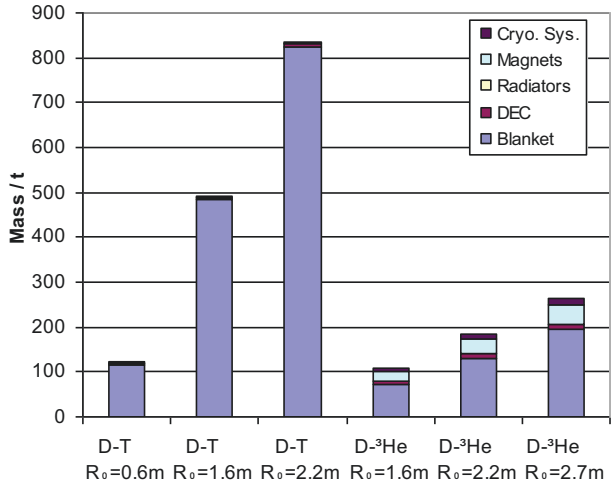

FIG. 5: *Mass breakdown of different ST fusion propulsion system configurations.*

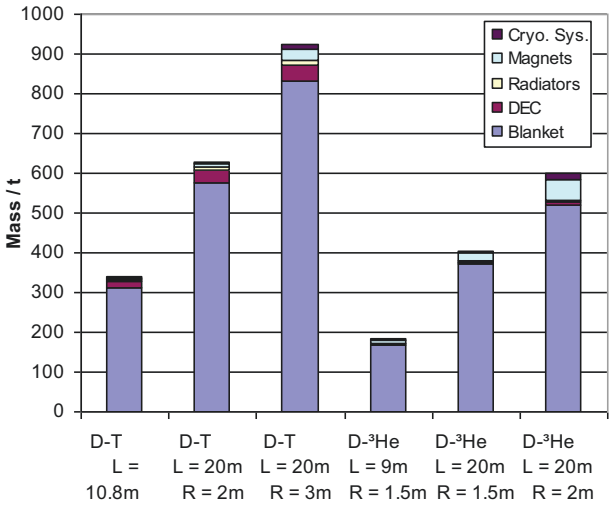

FIG. 6: *Mass breakdown of different FRC fusion propulsion system configurations*

α_{Rad} = 30 *kW/kg* are the respective mass-specific powers of the subsystems [12].
Assuming the use of superconducting electromagnets, the magnet subsystem mass m_{Mag} may be approximated using the virial theorem [12, 28]

$$m_{Mag} = \frac{C_{Mag}\rho_{sc}V_{Mag}B^2}{2\mu_0\sigma_{sc}}, \quad (16)$$

where ρ_{sc} = 2500 *kg/m^3*, and σ_{sc} = 10^9 *Pa* are the density and the upper stress limit of the superconductive material, respectively. The parameter μ_0 is the vacuum permeability and C_{Mag} = 2 a design safety factor. V_{Mag} is the total volume encompassed by the magnetic field coils. For all system designs discussed here, the magnets are assumed to be located at r_{Mag} = 0.5*m* from the first wall of the blanket. For D-³He reactors, this effectively corresponds to the magnets being fully located outside of the blanket, whereas for D-T systems the magnets are assumed to be embedded in the blanket at said position and thus within the DEC system, whose thickness in any case is assumed to be negligible. This design reduces the magnet mass and allows for a greater design range for the FRC system in particular, in which the relative radius between the plasma core and the magnets is of concern. The same layout was selected for the corresponding ST system in order to maintain a good comparison.

Obviously, a deeper investigation of the magnet's neutron load limits is required.
As it is for the blanket, the shape and mass of the magnetic coils are subject to the shape and physical properties of the plasma contained.
The cryogenic subsystem mass is roughly approximated by assuming

$$m_{Cryo} = \frac{m_{Mag}}{3}, \quad (17)$$

thus concluding the scope of the mass model. The total system mass m_{tot} corresponds to the sum of the blanket, DEC, radiator, magnet and cryogenic subsystem masses and may be used to derive mass specific power values suitable for a direct system comparison using eqn. (1).
TABs. 3 and 4 give an overview of the values obtained for the fusion propulsion system configurations based on the Spherical Tokamak and on the Field Reversed Configuration, respectively. FIGs. 5 and 6 present the mass composition of the individual configurations in visual form.

4.4 Discussion

Interesting result values pertaining to the absolute and mass-specific powers of the evaluated systems have been obtained, suggesting that the Spherical Tokamak and the

Field Reversed Configuration perform very differently depending mainly on the choice of fusion reactants. The highest power densities for an ST system were achieved assuming a D-^{3}He fusion plasma, with comparatively moderate results when utilising the more attainable D-T reaction. Contrastingly, downright spectacular absolute and relative thrust powers were obtained for an FRC system using D-T reactants, with far lower values when using the more advanced D-^{3}He fuel combination.
In general, the absolute thrust powers attained were very similar to those achieved and envisioned for the NERVA project, where the use of reactors yielding thrust powers of up to 5 *GW* had been considered, with the mass specific power values clearly falling short of this comparison due to the far lower system mass of a NERVA rocket engine [3]. However, the specific impulse I_{sp} and thus the exhaust velocity c_e achievable with the working gas propulsion systems discussed here can easily be expected to exceed any values established for fission-based solid core nuclear thermal propulsion systems considerably [11].
The absolute thrust power values determined for the evaluated system configurations are subject to the design condition requiring zero net power and dependent of both the plasma ion temperature T_i and the energy confinement time τ_E, which scales very differently for both confinement concepts (see eqns. (11) and (12)). τ_E directly and inversely affects the amount of thermal power losses. A high fusion power output is thus required in order to maintain a zero net power for small energy confinement times at a given temperature.
In general, the mass specific power of the ST fusion propulsion system is shown to be highly dependent on the reactor volume, with smaller reactors generally performing better while yielding only slightly reduced absolute thrust powers. In contrast, the mass specific power of FRC propulsion systems appears to be mostly independent of the plasma volume, enabling a straightforward rescaling to achieve a desired absolute thrust power.
It seems apparent that a fusion propulsion system based on the FRC, utilising a D-T reaction with effective propellant heating through the blanket is an excellent choice for missions requiring high thrust densities at short burn times, while burning fuels which can be readily obtained on Earth. However, a high coolant/propellant mass throughput is required to continuously absorb the high amount of reactor waste heat during burn times [12]. This suggests very limited burn times and that the system would be highly impractical for the execution of correctional manoeuvres requiring a limited Δv, especially when considering a most likely costly and tedious reactor start-up procedure.
When burning D-^{3}He fusion plasmas, the FRC systems evaluated appear to be clearly outperformed by their ST counterparts.
As the values for the approximate (sub-)system masses in TABs. 3 and 4 and their respective visualisations in FIGs. 5 and 6 suggest, working gas fusion propulsion systems in general are found to be considerably more massive for D-T fusion plasmas, which can almost exclusively be attributed to the use of a thicker blanket required to absorb higher neutron fluxes from the plasma core.
The maximum reasonable Earth-to-LEO (Low Earth Orbit) payload mass limit considered attainable using contemporary or near-future chemical rocket technology is ≈ 250*t*. Concerning the assembly of a fusion propelled spacecraft, the most sensible course of action would likely be to assemble individual modules in orbit, the design of which would require well-defined interfaces enabling an easy coupling of the modules [9].
A fusion propulsion system containing the subsystems considered in the mass model would most likely constitute a singular module. Bearing the payload mass constraint in mind, all but a very narrow range of feasible FRC systems prove too massive for mid-term space applications. Extrapolating from the data obtained for this study, one solution to this problem would be to select reactor design points with shorter coil lengths, reducing the overall mass without exceeding neutron and heat wall load limits due to the cylindrical geometry of the FRC. Regarding the ST propulsion system, most evaluated configurations operating on D-^{3}He fuel and a range of small D-T-burning systems appear to comfortably comply with the throwing mass constraint of launcher systems.

5. CONCLUSIONS AND OUTLOOK

The performances of two distinct magnetic confinement concepts, the Spherical Tokamak (ST) and the Field Reversed Configuration (FRC) were evaluated and compared with regards to their practical applicability as working gas nuclear fusion space propulsion systems using simple analytic models.
A simple fusion plasma performance model was coupled to two-dimensional solutions of the Grad-Shafranov equation corresponding to the respective confinement devices. Energy transport phenomena were modelled and a generalised Lawson criterion was adopted and applied resulting in a coarse analytic representation of a fusion reactor. Design points were selected specifically for the utilisation of the studied magnetic confinement fusion devices as fusion space propulsion systems, taking physical and practical constraints into account. The results were compared and discussed. The findings suggest that while fusion propulsion concepts operating on the grounds of the FRC principle operating with D-T fuel may offer potentially spectacular performances with regards to their mass specific and absolute thrust powers, ST propulsion systems may, however, be more manageable due a reduced absolute power yield, ST drives also appear to be the more realistic mid-term option, simply because of a generally lower overall system mass, particularly for small reactor sizes and when burning D-^{3}He reactants.
The models implemented for this study offer a variety of possibilities for future improvement. For example, the fidelity of the results regarding the performance of the fusion plasma may be enhanced by implementing a more sophisticated plasma model, incorporating ash and even impurities into the analysis rather than coarsely approximating their effects by enforcing simplistic particle multiples. As the model implemented here has merely been verified as being within an acceptable margin of error for Tokamak configurations, a more detailed examination of the subject might yield notable improvements of overall accuracy, especially with regards to results obtained for the FRC. Furthermore, issues pertaining to the necessary extraction of fusion products from the plasma were essentially ignored in this analysis.
While an effort was made to effectively adapt the generalised Lawson criterion presented in ref. [12] to a two-dimensional form, some aspects such as the

distribution of recuperated energy losses fed back into the fusion plasma were not dealt with.
The focus of this work lay on the application of the ST and the FRC as working gas drive fusion propulsion systems. Thus, no alternative concepts regarding the generation of thrust using these confinement concepts were explored in depth, neglecting a range of interesting options with potentially considerable effects on the overall system performance and mass.
The implemented mass model also leaves room for improvement. Some geometric properties, mainly the central column of the Spherical Tokamak have been mostly ignored in the analysis. While the column is expected to make up only a small fraction of the overall system mass, its position and relatively delicate structure are likely determining factors when assessing the fusion reactor's range of operation. The central column also houses the inboard part of the toroidal field coils, a fact which has not been considered in the approximation of the magnet mass in this study. Furthermore, potential constraints concerning the maximum neutron load of the superconductive magnet materials and subsequent implications for the shielding requirements were not explored in depth.
Other subsystems required to operate a working gas fusion propulsion system, such as those listed in section **4.3**, have been neglected from the mass approximation. Their inclusion may be worth or even necessary to consider for a more detailed analysis.
A deeper analysis of the performance for both of the discussed fusion propulsion systems may be conducted using data obtained and presented in this study, assuming a certain degree of fidelity of the results. While further figures of interest such as the propellant mass flow rate are only mentioned briefly on the side in this analysis, such values may be derived from the information given and applied to outline and specify ranges of possible mission scenarios for the ST and FRC working gas fusion propulsion systems respectively.

NOTE

Since the initial submission of this conference article in September 2013, the model presented here has been refined, especially with regards to the blanket modelling, yielding result values with a higher fidelity. The updated model as well as the results obtained therewith are presented and discussed in ref. [29].

ACKNOWLEDGEMENTS

All investigations towards this study have been performed at the Institute of Space Systems at the University of Stuttgart, Baden-Württemberg, Germany.

REFERENCES

[1] E. Messerschmid, S. Fasoulas: Raumfahrtsysteme – Eine Einführung mit Übungen und Lösungen. *Springer, Berlin, Heidelberg, 2004.*

[2] C. Williams: An Analytic Approximation to Very High Specific Impulse and Specific Power Interplanetary Space Mission Analysis. In: *Technical Report NASA Technical Memorandum 107058, 1996.*

[3] W. H. Robbins, H. B. Finger: A Historical Perspective of the NERVA Nuclear Rocket Engine Technology Program. In: *AIAA/NASA/OAI Conference on Advanced SEI Technologies, September 4-6, 1991 in Cleveland, Ohio, Lewis Research Center, AIAA 91-3451, 1991.*

[4] J. R. Roth: Introduction to Fusion Energy. *Ibis Publishing, 1986, ISBN: 0-935005-07-2*

[5] P-H. Rebut, D. Boucher, D. J. Gambier, B. E. Keen, M. L. Watkins: The ITER challenge. In*: Fusion Engineering and Design, Volume 22, Issues 1–2, 1993, pp. 7-18*

[6] V. K. Gusev, F. Alladio, A. W. Morris: The basics of spherical tokamaks and progress in European research. In: *Plasma Physics and Controlled Fusion 45 (2003), pp. A59-A82.*

[7] L. C. Steinhauer: Review of field-reversed configurations. In: *Physics of Plasmas 18 (2011).*

[8] M. Ono, S. M. Kaye, Y.-K.M. Peng, G. Barnes, W. Blanchard, M. D. Carter, J. Chrzanowski et al.: Exploration of spherical torus physics in the NSTX device. In: *Nuclear Fusion 40, no. 3Y (2000), pp. 557.*

[9] C. H. Williams, L. A. Dudzinski, S. K. Borowski, A. J. Juhasz: Realizing "2001: A space odyssey": Piloted spherical torus nuclear fusion propulsion. In: *Journal of spacecraft and rockets 39, no. 6 (2002), pp. 874-885.*

[10] N. N. Gorelenkov, L. E. Zakharov, M. Paluszek, and P. Bhatta: Magnetic Fusion Engine. In: *43rd AIAA/ASME/SAE/ASEE Joint Propulsion Conference & Exhibit, Cincinnati, OH, USA (2007)*

[11] R. A. Gabrielli, D. Petkow, G. Herdrich, H.-P. Röser: Two generic concepts for space propulsion based on thermal nuclear fusion. In: *63rd International Astronautic Congress, Naples, Italy (2012).*

[12] D. Petkow, R. A. Gabrielli, G. Herdrich, R. Laufer, H.-P. Röser: Generalized Lawson criterion for magnetic fusion applications in space. In: *Fusion Engineering and Design 87 (2012), pp. 30-39.*

[13] M. Tuszewsky: Review Paper Field Reversed Configurations. In: *Nuclear Fusion, Vol.28, no.11 (1988), pp. 2033-2092*

[14] W.T. Armstrong, R.K. Linford, J. Lipson, D.A. Platts and E.G. Sherwood: Field-reversed experiments (FRX) on compact toroids. In: *Phys. Fluids 24, no.11 (1981), pp. 2068-2089*

[15] Shafranov, V. D. Plasma equilibrium in a magnetic field. In: *Reviews of Plasma Physics, Vol. 2 (1966), New York: Consultants Bureau, pp. 103.*

[16] L. S. Solov'ev, Zh. Eksp. Teor. Fiz. 53, 626 (1967) [Sov. Phys. JETP 26, 400 (1968)]

[17] A. J. Cerfon, J. P. Freidberg: "One size fits all" analytic solutions to the Grad--Shafranov equation. In: *Phys. Plasmas 17, 032502 (2010)*

[18] L.C. Steinhauer: Improved analytic equilibrium for a field reversed configuration. In: *Phys. Fluids B, Vol.2, no. 12 (1990), pp.3081-3085*

[19] D. E. Post, R. V. Jensen, C. B. Tarter, W. H. Grasberger, W. A. Lokke: Steady-state radiative cooling rates for low-density, high-temperature plasmas. In: *Atomic data and nuclear data tables 20, no. 5 (1977), pp. 397-439*.

[20] M. Keilhacker, A. Gibson, C. Gormezano, P. J. Lomas, P. R. Thomas, M. L. Watkins, P. Andrew et al.: High fusion performance from deuterium-tritium plasmas in JET. In: *Nuclear Fusion 39, no. 2 (1999), pp. 209.*

[21] C. M. Roach, M. Walters, R. V. Budny, F. Imbeaux, T. W. Fredian, M. Greenwald, J. A. Stillerman et al.: The 2008 Public Release of the International Multi-tokamak Confinement Profile Database. In: *Nuclear Fusion 48, no. 12 (2008) 125001.*

[22] H. Momota, O. Motjima, M. Okamoto, S. Sudo, Y. Tomita, S. Yamaguchi, A. Iiyoshi, M. Onozuka, M. Ohnishi, C.

Uenosono: Characteristics of D-^{3}He fueled FRC Reactor: ARTEMIS-L. In: *National Institute for Fusion Science, Japan, 1993.*

[23] R. L. Miller, The ARIES Team: ARIES-ST design point selection. In: *Fusion Engineering and Design 65, no. 2 (2003), pp. 199-213.*

[24] H.-S. Bosch, G. M. Hale: Improved formulas for fusion cross-sections and thermal reactivities. In: *Nuclear Fusion 32, no. 4 (1992), pp. 611-631.*

[25] F. Najmabadi, The ARIES Team: Spherical torus concept as power plants - the ARIES-ST study. In: *Fusion Engineering and Design 65, no. 2 (2003): pp. 143-164.*

[26] M. Greenwald, J. L. Terry, S. M. Wolfe, S. Ejima, M. G. Bell, S. M. Kaye, G. H. Neilson: A new look at density limits in tokamaks. In: *Nuclear Fusion 28, no. 12 (1988): 2199.*

[27] L. Giancarli, J. Bonal, A. Caso, G. Le Marois, N. Morley, J. Salavy: Design requirements for SiC/SiC composites structural material in fusion power reactor blankets. In: *Fusion Engineering and Design 41 (1998), pp. 165–171.*

[28] T. Kammash, M. Lee, D. Galbraith, B. Cassenti, S. Borowski, R. Bussard, et. al.: Fusion energy in space propulsion. In: *AIAA – Progress in Astronautics and Aeronautics, vol. 167, 1995.*

[29] A. S. Pagan, E. Ferrer Gil, R. A. Gabrielli, G. Herdrich: Comparative Assessment of Spherical Tokamak and Field Reversed Configuration Nuclear Fusion Space Propulsion Systems. Submitted to *Fusion Engineering and Design* in October 2013